Aeroacoustic response of coaxial wall-mounted Helmholtz resonators in a low-speed wind tunnel

William V. Slaton[a)]
Department of Physics and Astronomy, The University of Central Arkansas, 201 Donaghey Avenue, Conway, Arkansas 72035-0001

Asami Nishikawa
Department of Physics and Astronomy, The University of Mississippi, 108 Lewis Hall, University, Mississippi 38677-1848

(Received 7 May 2014; revised 9 November 2014; accepted 12 November 2014)

The aeroacoustic response of coaxial wall-mounted Helmholtz resonators with different neck geometries in a low-speed wind tunnel has been investigated. Experimental test results of this system reveal a strong aeroacoustic response over a Strouhal number range of 0.25 to 0.1 for both increasing and decreasing the flow rate in the wind tunnel. Aeroacoustic response in the low-amplitude range $O(10^{-3}) < V_{ac}/V_{flow} < O(10^{-1})$ has been successfully modeled by describing-function analysis. This analysis, coupled with a turbulent flow velocity distribution model, gives reasonable values for the location in the flow of the undulating stream velocity that drives vortex shedding at the resonator mouth. Having an estimate for the stream velocity that drives the flow-excited resonance is crucial when employing the describing-function analysis to predict aeroacoustic response of resonators. © *2015 Acoustical Society of America*.
[http://dx.doi.org/10.1121/1.4904521]

[RR] Pages: 253–260

I. INTRODUCTION

Aeroacoustic excitation of Helmholtz resonators is music to the ears of many researchers. This work focuses on the flow-induced resonance of coaxial wall-mounted Helmholtz resonators in a low-speed wind tunnel. Selected references to work on single Helmholtz resonators excited by flow relevant to this paper include: Cummings[1] proposed feed-back loop-gain criteria to analyze blowing over a wine bottle, Anderson[2] and Elder[3–5] presented extensive velocity and pressure measurements on a wall-mounted resonator in addition to loop-gain theory for self-excitation, Howe[6,7] presents a detailed theoretical treatment of self-sustained cavity oscillations, Nelson and colleagues[8,9] present companion papers with detailed flow visualization and acoustics measurements of a wall-mounted Helmholtz resonator. The detailed frequency and acoustic measurements of Nelson *et al*. provide data for future modeling efforts using loop-gain criteria by Mast and Pierce[10,11] that is the analysis used in this work. Further measurements on flow-excited resonance and the use of loop-gain criteria for analysis are presented by Meissner[12,13] in a series of papers. Computational fluid dynamics techniques have been used to explore a flow's excitation of a Helmholtz resonator mainly to understand automobile buffeting.[14–19]

Also of interest to this work are measurements of the impedance of Helmholtz resonators in the presence of grazing flow. The interaction of the flow in the wind tunnel with the oscillating cross-flow from the Helmholtz resonator is complex. Walker and Charwat[20] combine measurements with numerical simulations to propose a "hinged-lid" model for resonator's in-flow and out-flow into the wind-tunnel's stream. This "hinged-lid" model is further investigated by Cummings.[21] Peat *et al*.[22] compare theoretical models to experiments of the impedance of circular-orifice Helmholtz resonators in the presence of grazing flow.

The effect of a Helmholtz resonator's geometry on flow-induced excitation is contained within the review of Rockwell and Naudascher,[23] Panton,[24] and extensive theoretical, numerical and experimental work by Dequand *et al*.[25,26] Flow-induced excitation of coaxial straight side-branches is also important for this work because we will investigate the aeroacoustic response of coaxial Helmholtz resonators. Important works relevant to coaxial side branches are by Bruggeman *et al*.[27] and Kriesels *et al*.[28] in which very high amplitude acoustic oscillations are measured and continued by Ziada,[29,30] Meissner,[32] and Oshkai *et al*.[33] Measurements of the aeroacoustic source power available in a coaxial side-branch configuration utilizing a damper within the side-branch was done by Slaton and Zeegers.[31]

The work described in this paper examines the aeroacoustic excitation of coaxial wall-mounted Helmholtz resonators in a low-speed wind tunnel. The purpose is to evaluate this configuration for its ability to interact with the mean flow to excite and sustain resonance and to compare the measured low-amplitude aeroacoustic response to a describing-function model introduced by Mast and Pierce.[11] The Helmholtz resonator's frequency can be easily changed by modifying the neck length. In this way, we will explore the aeroacoustic excitation over a range of flow rates and resonance frequencies. An added benefit of using a Helmholtz resonator is that its fundamental frequency is not directly related to its higher harmonics. Hence nonlinear

[a)]Author to whom correspondence should be addressed. Electronic mail: wvslaton@uca.edu

wave steepening and higher harmonic generation in standing-wave side-branch systems is avoided. The experimental setup used in this investigation is described in detail in Sec. II. The experimental results of the investigation are found in Sec. III with an analysis in Sec. IV. Conclusions may be found in Sec. V.

II. EXPERIMENTAL APPARATUS

In this section, we detail the experimental setups used to investigate the aeroacoustic response of coaxial wall-mounted Helmholtz resonators. A low pressure vacuum system capable of a maximum speed of 28 m/s is connected to an empty 2-in. inner diameter, wind tunnel as illustrated in Fig. 1. Connections between glass and plastic elements are made with standard Schott[34] couplings. Variable flow rate is provided by connecting the vacuum to a variable transformer. The wind tunnel draws in ambient air down the 1.81-m straight section. According to Narayana,[35] a fully developed turbulent velocity profile has formed after inflow in a duct of diameter, D, when the distance down the duct exceeds the entrance length, L_e, given by

$$L_e = 4.4\mathrm{Re}^{1/6}D, \tag{1}$$

where $\mathrm{Re} = V_{flow}D\rho/\mu$ is the Reynolds with the air's density and viscosity given by ρ and μ respectively and V_{flow} is the flow velocity of the air in the center of the wind tunnel. For our set up, $L_e \sim 1.5$ m at the highest wind tunnel flow speed. Hence we are assured a fully formed velocity profile has developed within the wind tunnel before the site of aeroacoustic excitation occurs. For our lowest value of V_{flow}, which results in aeroacoustic excitation of the system, $\mathrm{Re} \sim 33\,000$, which is in the turbulent regime.

Referring to Fig. 1, the inflowing air velocity is measured with a pitot tube that is visually aligned and centered in the wind tunnel in 2-in. Delrin plastic couplings. The pitot tube utilizes a differential pressure sensor[36] and was calibrated using an Omega HHF92A digital airflow/temperature meter, which has a resolution of 0.01 m/s over our range of interest. The output of the pitot tube was read by a 175 Fluke true rms multimeter. Connected to the pitot tube is a 2-in. ID glass cross-junction of length 19.6 cm and width 19.6 cm. The internal edges of the cross-junction are rounded to a radius of curvature of approximately 1/4 in. Following the cross-junction is an Omega HH501DK K-type thermocouple

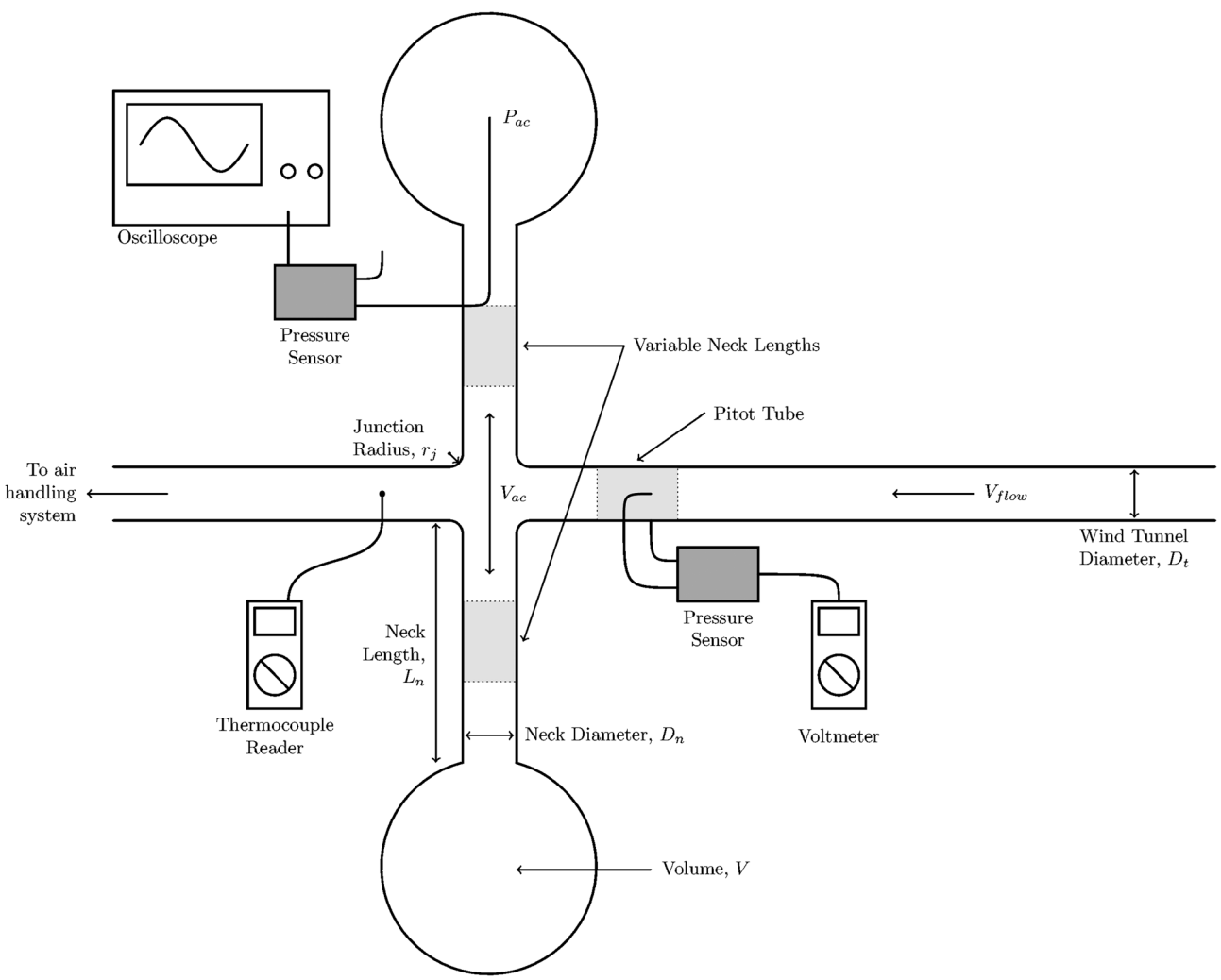

FIG. 1. Overview of aeroacoustic wind tunnel setup with coaxial wall-mounted side branches composed of straight equal neck length Helmholtz resonators. The variable neck lengths used in this experiment can be found in Table I.

to measure air temperature positioned in the center of the flow. Next, a 0.75 m long section of 2-in. ID glass pipe connects the wind tunnel to a ~3 m flexible hose with ~2-in. inner diameter, which is connected to the vacuum system. Cotton cloth placed over the junction between the wind tunnel and flexible hose acts as a muffler for high frequency noise from the vacuum system.

Aeroacoustic excitation of the system occurs at the cross-junction. Attached to the cross-junction are side branches that comprise the resonant acoustic system of interest. The side branch configuration is illustrated in Fig. 1 where the effective neck length of the flask is changed by adding straight 2-in. inner diameter Delrin plastic couplings between the cross-junction and the 5 l flasks.[37] The actual lengths of the plastic couplings are within 0.3 cm of the stated length due to machining process. For all the data presented, the lengths of both side branches are equal. The flasks have a neck length of 9.30 cm and an inner neck diameter of 2 in.

Acoustic pressure oscillations in one of the 5 l flasks was measured with another differential pressure sensor[36] that was calibrated with a water manometer and acts as a high amplitude microphone. The pressure sensor is connected to a 30-cm long, 1/32-in. inner diameter, brass tube bent into an L-shape with a radius of curvature of 1/2 in. that enters at the coupling at the mouth of one of the flasks and extends along the center of the neck duct to the center of the flask. Viscous/thermal losses within this tube are accounted for. The output of the microphone is read by a Hewlett Packard 54 663P oscilloscope, which gave reliable peak to peak voltage and frequency readings. Acoustic readings in the flask were cleanly sinusoidal and did not display nonlinear effects for any experimental runs. This indicates the pressure sensor was not driven too hard and that nonlinear acoustic wave-steepening effects, if present, were not noticeable.

III. EXPERIMENTAL RESULTS

Before the experimental data collected from the aforementioned experimental setup can be presented we need to introduce some useful relationships between the measured quantities. The Strouhal number is a convenient nondimensional number for characterizing aeroacoustic phenomena. It is defined as

$$St = \frac{fW_{eff}}{V_{flow}}, \tag{2}$$

where f is the sounding frequency of the periodic phenomena (the shedding of vortices or equivalently the frequency of the acoustic wave), W_{eff} is the effective width or diameter of the side branch opening to the wind tunnel, and V_{flow} is the flow velocity of the air in the wind tunnel. The authors chose the flow velocity to be that measured by the pitot tube in the center of the wind tunnel. Care must be taken when reviewing the literature for flow-induced resonance because this choice is not universal. The effective diameter of the circular side branch pipe with rounded edges joining the circular wind tunnel duct at the cross-junction is defined as[38]

$$W_{eff} = \frac{\pi}{4} D_s + r_j, \tag{3}$$

with D_s as the diameter of the side branch and r_j is the radius of curvature of the upstream edge of the mouth of the junction.[28]

This experiment examines the aeroacoustic response of identical coaxial wall-mounted Helmholtz resonators connected to a low-speed wind tunnel. A Helmholtz resonator has a fundamental acoustic frequency, f_H, defined by

$$f_H = \frac{c}{2\pi}\sqrt{\frac{S_H}{V_H L'_H}}, \tag{4}$$

where c is the ambient speed of sound, S_H is the cross-sectional area of the resonator's neck, V_H is the volume of the resonator's cavity, and L'_H is the effective length of the neck. The effective neck length for a Helmholtz resonator with a neck flanged on both ends[39,40] is, $L'_H = L + 1.7D_s/2$ where D_s was defined previously. The only convenient variable to change in the setup that affects the frequency is the length of the resonator necks. For all experiments reported here, these neck lengths are equal on each side of the wind tunnel.[41]

Treating the Helmholtz resonator as a simple mass-spring system results in the measured acoustic pressure oscillations in the flask to be 90° out of phase with the acoustic velocity of the gas in the resonator neck. By considering sinusoidal oscillations for an ideal Helmholtz resonator, the acoustic velocity amplitude in the neck of the resonator can be related to the acoustic pressure amplitude in the flask as

$$V_{ac} = \frac{V_H \omega}{\rho_0 c^2 S_H} P_{ac}, \tag{5}$$

where ρ_0 is the ambient air density inside the wind tunnel, $\omega = 2\pi f$, P_{ac} is the acoustic pressure amplitude, and the other variables have already been defined. A useful dimensionless ratio is V_{ac}/V_{flow}, which represents the ratio of the oscillating acoustic flow velocity to the flow velocity at the center of the wind tunnel before the cross-junction.

The aeroacoustic response of the system described in Sec. II utilizing the 5 l flasks and 2-in. inner diameter necks of varying length will now be presented. The frequency response of the resonators is displayed in Figs. 2 and 3. Figure 2 shows the measured sounding frequency as a function of the Strouhal number, St. Open symbols indicate data taken while the flow in the wind tunnel is increasing from zero. Closed symbols are data taken while the flow in the wind tunnel is decreasing from the maximum of 28 m/s. We observe very slight changes in the resonator sounding frequency over the range of aeroacoustic excitation. As the data indicates, we observe strong excitation of the resonators over a wider flow range for higher frequencies than for lower frequencies.

Figure 3 displays the average sounding frequency for a given neck length along with the theoretical prediction for a

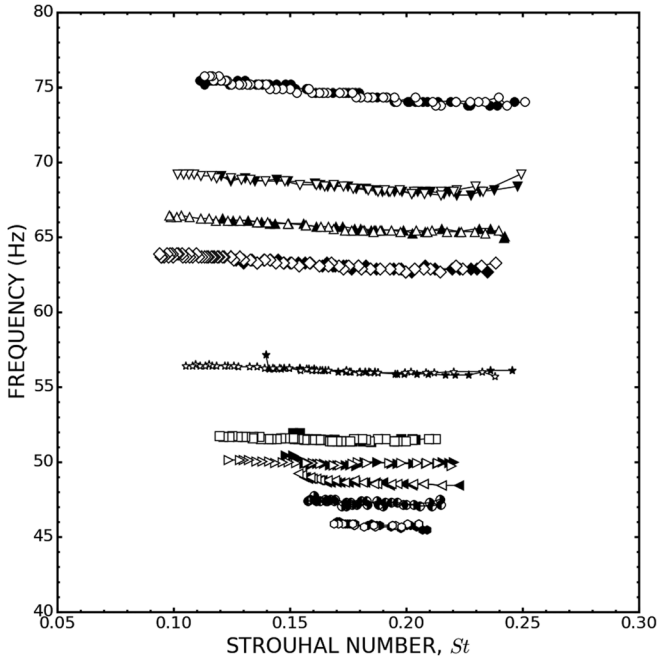

FIG. 2. Sounding frequency vs Strouhal number of coaxial wall-mounted Helmholtz resonators with different neck lengths as denoted in Table I. Open symbols denote data taken when the flow is increasing from zero. Closed symbols are data taken while for flow in the wind tunnel is decreasing from the maximum of 28 m/s.

Helmholtz resonator as expressed in Eq. (4). We see better agreement between the simple models at lower frequencies than at higher frequencies. In terms of our simple mass-spring model, higher actual frequencies means either the Helmholtz neck length is shorter than measured or the effective cross-sectional area of the neck is less. According to the "hinged-lid" model of Ref. 21, our low-speed wind tunnel coupled to our low-frequency resonators keeps us in the "wall separation regime." This means that the viscous boundary layer detaches from the wind-tunnel wall at a point up stream that is greater than the diameter of the neck opening. This implies that the effective neck area is not changed for our experiment. However, Ref. 22 shows measurements of the effective end correction for the resonator neck as a function of a scaled Strouhal number. When applied to our experiment, Ref. 22 implies that the effective end correction should be about half what was used in L'_H and partially explains the discrepancy between the measurements and the simple model used here at higher frequencies. That is, at higher frequencies (i.e., shorter necks), the correction is a greater percent of the total neck length and is therefore a larger influence on these frequencies than longer neck lengths (i.e., lower frequencies). Further work needs to be done to quantify the end-correction for wall-mounted resonators in flow.

The aeroacoustic excitation of the straight coaxial Helmholtz resonator necks as the flow is increased and decreased is displayed in Figs. 4 and 5. These figures display the ratio of the acoustic velocity at the site of vortex shedding divided by the flow velocity, V_{AC}/V_{flow}, at the center of the wind tunnel vs the Strouhal number, St. Data in these figures follow the same convention as in previous figures, open symbols are for measurements when the flow in the wind tunnel is increasing from zero and closed symbols are when the wind tunnel flow is decreasing from its maximum value of 28 m/s. Figure 5 is illustrative of the resonator's performance: As the wind tunnel flow rate is increased, the first

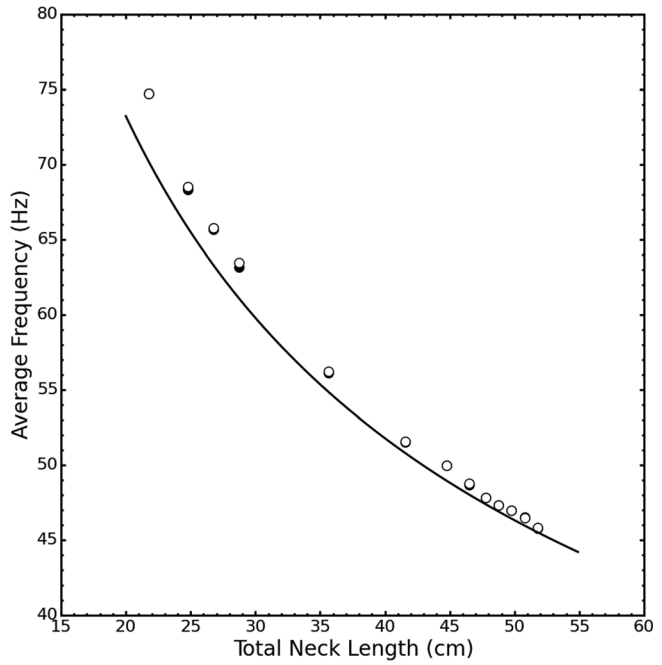

FIG. 3. The average sounding frequency for all individual neck lengths displayed in Fig. 3 vs the variable neck length. Solid line is simple Helmholtz resonator frequency from Eq. (4). Open symbols are the average of the frequencies measured while increasing the flow. Closed symbols (mostly obscured) are the average of the frequencies measured while decreasing the flow from its maximum.

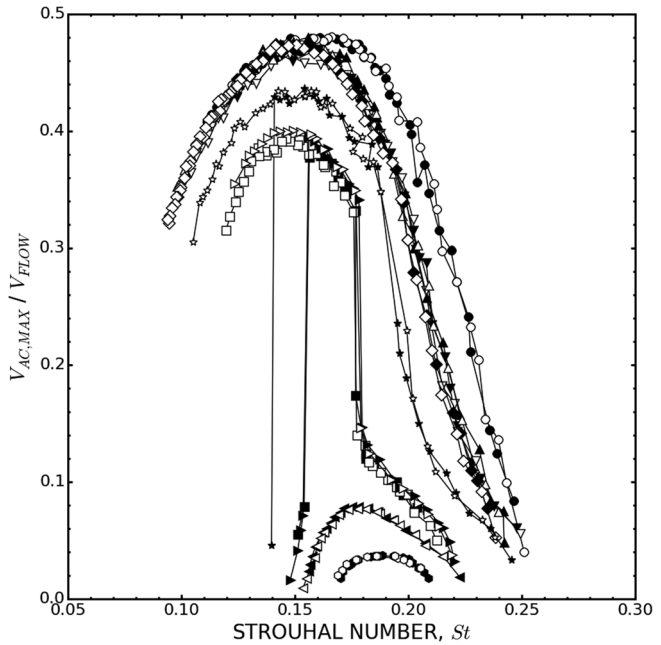

FIG. 4. The ratio of the acoustic velocity amplitude, V_{ac}/V_{flow}, vs the Strouhal number, St, for coaxial wall-mounted Helmholtz resonators with neck lengths displayed in Table I. Open symbols denote data taken when the flow is increasing from zero. Closed symbols are data taken while for flow in the wind tunnel is decreasing from the maximum of 28 m/s.

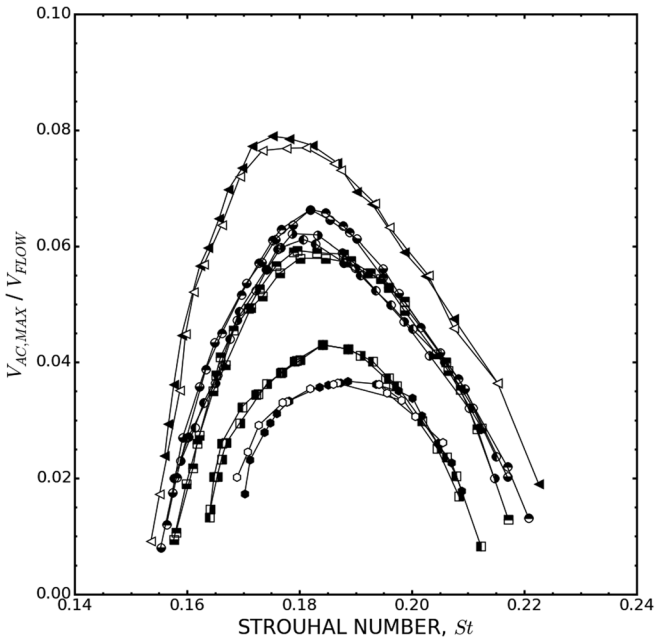

FIG. 5. Detail of the acoustic velocity amplitude ratio data for long coaxial Helmholtz resonator neck lengths displayed in Table I not all displayed in Fig. 4. Open symbols denote data taken when the flow is increasing from zero. Closed symbols are data taken while for flow in the wind tunnel is decreasing from the maximum of 28 m/s.

detected acoustic excitation of the resonator is found between $0.2 < St < 0.25$. As the flow rate is increased, the acoustic pressure amplitude response in the resonator flask climbs quickly to a maximum value. Shorter neck lengths reach higher acoustic amplitudes. We see a dramatic, bell-shaped curve because once the acoustic excitation amplitude has saturated, increases in the flow rate decrease the ratio V_{ac}/V_{flow}. A summary of the data for various neck lengths in found in Table I. Upon reaching this maximum, further increases in flow rate tend to decrease the acoustic response until there is a sudden disappearance of the acoustic resonance. Similar abrupt changes in acoustic signal were reported by Ziada in Refs. 29 and 30 among others. Starting the flow at high flow rate and slowly decreasing it results in the filled data symbols. As can be seen, the flow excited resonance "kicks in" at a different flow rate than when it shut off when the flow was increasing.

Figure 4 displays only two of the longer neck lengths for comparison purposes; more are displayed in Fig. 5. Here the acoustic response of the system is lower and does not display abrupt changes except in the 25 cm neck length data. Of interest is the range of excitation: The longest necks have a response that falls within the range of $O(10^{-3}) < V_{ac}/V_{flow} < O(10^{-1})$, which enables analysis with the describing-function theory described by Anderson,[2] Elder,[3,4] Mast and Pierce,[10,11] and Meissner.[12,13] The shortest neck lengths reach velocity ratios near 0.5, which is impressive for this wind tunnel operating near atmospheric pressure.

TABLE I. Compilation of measured wind tunnel flow velocity, V_{flow}^{max}, sounding frequency, f, maximum acoustic pressure amplitude in the flask, P_{ac}^{max}, at maximum acoustic velocity ratio, V_{ac}/V_{flow} for the listed variable neck lengths. Data symbols as they appear in the data plots are also listed. Open symbols denote data taken when the flow is increasing from zero. Closed symbols are data taken while for flow in the wind tunnel is decreasing from the maximum of 28 m/s.

Neck type	Plot symbol	Flow	V_{flow}^{max} (m/s)	f (Hz)	P_{ac}^{max} (Pa)	V_{ac}^{max}/V_{flow}
0 cm	Filled circle	Decreasing	21.4	74.6	1153.0	0.48
0 cm	Open circle	Increasing	20.8	74.6	1118.2	0.48
3 cm	Filled down triangle	Decreasing	19.7	68.6	1132.2	0.47
3 cm	Open down triangle	Increasing	21.5	68.7	1219.0	0.465
5 cm	Filled up triangle	Decreasing	19.6	65.9	1192.2	0.48
5 cm	Open up triangle	Increasing	20.5	65.9	1226.4	0.472
7 cm	Filled diamond	Decreasing	18.7	63.3	1174.9	0.475
7 cm	Open diamond	Increasing	19.4	63.3	1217.4	0.474
14 cm	Filled star	Decreasing	16.9	56.3	1095.1	0.437
14 cm	Open star	Increasing	18.2	56.3	1179.1	0.435
20 cm	Filled square	Decreasing	15.1	51.5	959.1	0.39
20 cm	Open square	Increasing	16.3	51.6	1042.4	0.394
23 cm	Filled right triangle	Decreasing	14.8	49.9	980.5	0.395
23 cm	Open right triangle	Increasing	15.5	50.0	1038.6	0.401
25 cm	Filled left triangle	Decreasing	12.8	48.7	174.5	0.079
25 cm	Open left triangle	Increasing	12.4	48.7	164.5	0.077
26 cm	Top filled circle	Decreasing	12.1	47.7	141.1	0.066
26 cm	Bottom filled circle	Increasing	12.1	47.7	141.1	0.066
27 cm	Left filled circle	Decreasing	12.1	47.4	131.0	0.061
27 cm	Right filled circle	Increasing	12.2	47.2	134.6	0.062
28 cm	Top filled square	Decreasing	12.1	46.8	127.8	0.059
28 cm	Bottom filled square	Increasing	12.1	47.0	124.6	0.058
29 cm	Left filled square	Decreasing	11.7	46.5	90.5	0.043
29 cm	Right filled square	Increasing	11.7	46.5	90.5	0.043
30 cm	Filled hexagon	Decreasing	11.2	45.8	75.3	0.037
30 cm	Open hexagon	Increasing	11.3	45.7	75.3	0.036

IV. ANALYSIS

We will use the describing-function theory as laid out in the work by Mast and Pierce[11] to model the resonator response data in the range $O(10^{-3}) < V_{ac}/V_{flow} < O(10^{-1})$. In this low-amplitude range, it is thought that the pressure fluctuation associated with flow disturbances is proportional. This pressure fluctuation, P_{drive}, is related to a flow velocity near the duct wall, V_{wall}, in the wind tunnel via

$$P_{drive} = \beta \rho V_{wall}^2, \tag{6}$$

where β is a constant. As noted by Mast,[10] the Helmholtz resonator's quality factor, Q, acts as an amplifier of P_{drive} yielding the measured acoustic pressure amplitudes in the flask during flow-excited resonance. In this way, the values in Table I may be used in this expression for β,

$$\beta = \frac{P_{ac}^{max}}{\rho V_{\substack{max\\wall}}^2 Q_0}, \tag{7}$$

where Q_0 is the quality factor of the resonator at max response, $Q_0 = \sqrt{KM}/R_0$, where $K = \rho c^2 S_H^2/V_H$, $M = \rho S_H L'_H$, and R_0 is the radiation resistance of a baffled source at resonance, $R_0 = \rho c (k_0 S_H)^2/2\pi$ with $k_0 = \omega_0/c$ where ω_0 is the resonators angular resonance frequency given by $\omega_0 = \sqrt{K/M}$. At other frequencies, R will vary as $(kD_s/2)^2$ like a piston in a baffle.

We refer the reader to Ref. 11 for a full description of describing-function theory and its application to flow-excited resonators. What follows is a quick review how the flow-excited resonator responds to and is influenced by a flow disturbance in the wind tunnel's boundary layer. Reference 11 argues that the forward gain function which drives the resonator is given by

$$\left(\frac{q_o}{q_r}\right)_{forward} = \frac{\beta S_H^2 \rho V_{wall}^2}{\omega M |q_r|} e^{-i\left(3\pi/2 - 2\omega W_{eff}/V_{wall}\right)}, \tag{8}$$

where q_r is the *resonator* volume velocity. q_o is the *orifice* volume flow, which is "the flow that would occur in the absence of any resonator for a given pressure disturbance across the orifice." The sum, $q_r + q_o = q_{total}$, represents the total volume flow into the resonator. At resonance, q_r is approximately equal to q_{total}. The backward gain function describes the resonator's response to excitation to the flow disturbance. Reference 11 treats the Helmholtz resonator as a driven damped mass-spring system,

$$(-\omega^2 M - i\omega R + K)x = S_H P_{drive}(x,t), \tag{9}$$

where x is the average displacement of the fluid in the resonator neck, which, for simple harmonic motion, is related to the volume velocity of the fluid in the resonator neck as $q_{total} = -i\omega S_H x$. Hence using $q_r + q_o = q_{total}$, Eq. (9) can be written as

$$q_r = \frac{(K - i\omega R) S_H^2 P_{drive}}{i\omega M (K - M\omega^2 - i\omega R)}. \tag{10}$$

The backward gain function can be defined by utilizing Eq. (10) and $q_o = p_{drive}/(-i\omega M)$ to give

$$\left(\frac{q_r}{q_o}\right)_{backward} = \frac{1 - i\omega R/K}{\left(\omega/\sqrt{K/M}\right)^2 - (1 - i\omega R/K)}, \tag{11}$$

or, in terms of nondimensional variables, $\Omega = \omega/\omega_0$ and the quality factor $Q = \sqrt{KM}/R$, the backward gain function is

$$\left(\frac{q_r}{q_o}\right)_{backward} = \frac{1 - i\Omega/Q}{\Omega^2 - (1 - i\Omega/Q)}. \tag{12}$$

Stable self-excited oscillations require that the product of the forward and backward gain functions be identically one, hence,

$$\left(\frac{q_o}{q_r}\right)_{forward} \left(\frac{q_r}{q_o}\right)_{backward} = 1. \tag{13}$$

For a given velocity near the wall, V_{wall}, and resonator dimensions, this equation's real and imaginary parts yield two equations for the unknown resonator neck velocity response, $|q_r|$ and its frequency of oscillation, ω. Our method of solution for $|q_r|$ and ω parallels that of Ref. 11. Plugging Eqs. (8) and (12) into the loop-gain criteria of Eq. (13) yields

$$\frac{\beta S_H^2 \rho V_{wall}^2}{\omega M |q_r|} e^{-i\left(3\pi/2 - 2\omega W_{eff}/V_{wall}\right)} \frac{1 - i\Omega/Q}{\Omega^2 - (1 - i\Omega/Q)} = 1. \tag{14}$$

This expression implies that the imaginary part of the loop gain is zero, hence,

$$\mathrm{Im}\left[e^{-i\left(3\pi/2 - 2\omega W_{eff}/V_{wall}\right)} \frac{1 - i\Omega/Q}{\Omega^2 - (1 - i\Omega/Q)}\right] = 0. \tag{15}$$

Following a procedure of expanding the exponential and rationalizing the denominator as described by Ref. 11 yields the following for the imaginary part,

$$2\left(\frac{\omega W_{eff}}{V_{wall}}\right) = \tan^{-1}\left(\frac{Q^2 - \Omega^2(Q^2 - 1)}{\Omega^3 Q}\right) + 2n\pi, \tag{16}$$

where n is an integer. The case $n = 1$ corresponds to the highest-amplitude oscillations of a flow-excited resonator, which is the case for this paper and Ref. 11. The preceding equation with the other quantities as defined before can be numerically solved for ω for a specified value of V_{wall}. Then the value of ω is used in Eq. (14), which yields a value for the resonator volume velocity, $|q_r|$. Last, the total volume velocity response in the resonator neck can be determined via

$$|q_{total}| = |q_r||1 + (q_r/q_o)^{-1}_{backward}|. \tag{17}$$

It should be noted that we measure the flow velocity in the center of the wind tunnel before the junction. This flow

velocity is related to V_{wall} via $V_{wall} = V_{flow}/s$ where s is a scale factor. With this addition, Eq. (7) now depends on s: $\beta = (s^2 P_{ac}^{max})/(\rho V_{flow\,max}^2 Q_0)$. This expression for β can be incorporated into Eq. (14) and used to fit the theory to the measured data.

For each neck the response of which is in the range $O(10^{-3}) < V_{ac}/V_{flow} < O(10^{-1})$, we run a PYTHON program written to solve the equations in the preceding text for ω and q_{total}/S_H for the given geometry of the system by adjusting the value of the scale factor, s, until a good fit of the theory to the data is found. Table I summarizes the values of P_{ac}^{max} and V_{flow}^{max} used in the determination of β. Minor adjustments of the effective lengths of the resonator necks (typically less than 5 mm, which is less than 1% of the total neck length) was also used to better match theoretical predictions for the sounding frequency to the measured data. Sounding frequency vs Strouhal number, St, for the measured data and theoretical predictions are displayed in Fig. 6. We can see that the describing-function model for the flow-excited resonator reasonably predicts the sounding frequency of the resonator. The ratio V_{ac}/V_{flow} vs Strouhal number, St, for the measured data and the theoretical prediction is displayed in Fig. 7. These data were used to adjust the scale parameter, s, to reasonably fit the data. The scale factor primarily adjusts the theoretical curve for sounding frequency and velocity ratio to the left and right with small changes vertically through the parameter, β.

All neck lengths with a response in the range $O(10^{-3}) < V_{ac}/V_{flow} < O(10^{-1})$ were analyzed, but only the extremes are plotted for clarity. The numerical value of the scale factor ranges from 2.58 for the +30 cm neck to 2.75 for the +25 cm neck when fitting with the values of P_{ac}^{max} and V_{flow}^{max} found when the wind tunnel's flow rate is increasing. These scale numbers are comparable to those found by Howe[6] for a vortex street excited Helmholtz resonator. As determined earlier, it is a safe assumption that the flow is turbulent in the wind tunnel leading to the junction because the Reynolds number, $\mathrm{Re} = D_{pipe} V_{flow} \rho/\mu$ is $\sim 33\,000$ at a wind tunnel flow speed of 10 m/s, which is typical for aeroacoustic excitation of the low-frequency resonators in the range $O(10^{-3}) < V_{ac}/V_{flow} < O(10^{-1})$.

A well-established model[42,43] for turbulent velocity profile in pipes that conforms well to data with $\mathrm{Re} > 20\,000$ is known as the *logarithmic distribution*. The logarithmic distribution, with appropriate approximations, can be used to demarcate three regions in the flow: the viscous sublayer, the buffer zone, and the turbulent core. Using the measured V_{flow}^{max} and fitted scale factor, s, allows us to estimate the location of the fluctuating boundary layer, V_{wall}, that drives the aeroacoustic response of these low-frequency resonators. It is found that the location of the driving force within the wind tunnel exciting the resonators is approximately 1 cm from the tube wall. In terms of the logarithmic distribution, this location lies outside of the buffer zone and partially in the turbulent core which is reasonable for this system.

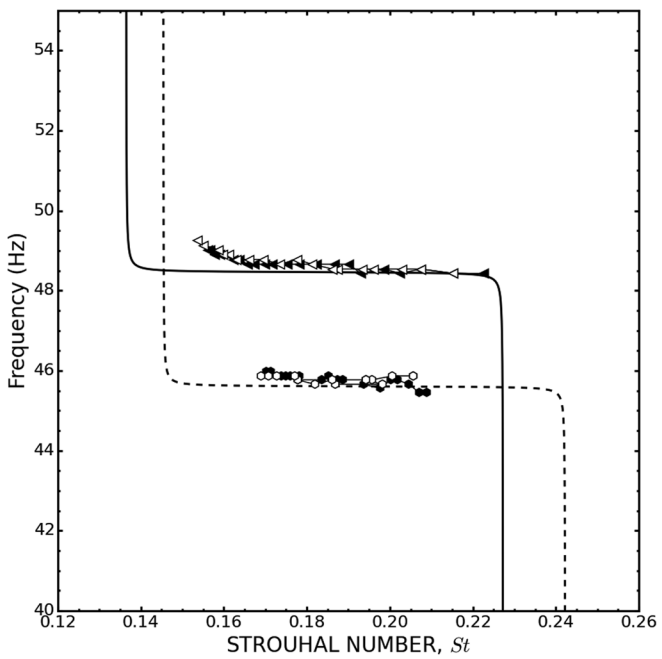

FIG. 6. Measured sounding frequencies vs Strouhal number for the +25 and +30 cm variable neck length resonators. Open symbols denote data taken when the flow is increasing from zero. Closed symbols are data taken while for flow in the wind tunnel is decreasing from the maximum of 28 m/s. The solid and dotted lines are the result of using the describing-function model of Ref. 11 with a scaling factor of $s = 2.58$ for the +30 cm resonator and $s = 2.75$ for the +25 cm resonator variable neck length.

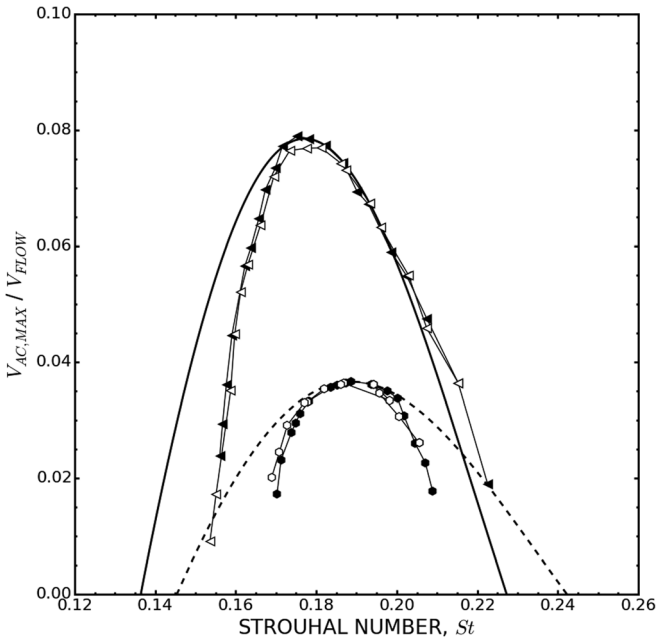

FIG. 7. Measured acoustic velocity amplitude ratio, V_{ac}/V_{flow} vs Strouhal number, St, for the +25 and +30 cm variable neck length resonators. Open symbols denote data taken when the flow is increasing from zero. Closed symbols are data taken while for flow in the wind tunnel is decreasing from the maximum of 28 m/s. The solid and dotted lines are the result of using the describing-function model of Ref. 11 with a scaling factor of $s = 2.58$ for the +30 cm resonator and $s = 2.75$ for the +25 cm resonator variable neck length.

V. CONCLUSIONS

In this work, we describe a low-speed wind tunnel with coaxial variable neck-length Helmholtz resonators. Extensive experimental test results of this system reveal strong aeroacoustic response over a Strouhal number range of

0.1–0.25 for both increasing and decreasing the flow rate in the wind tunnel with some hysteresis present. Ninety-degree bends in the resonator necks does not significantly change the aeroacoustic response of the system. Aeroacoustic response in the low-amplitude range $O(10^{-3}) < V_{ac}/V_{flow} < O(10^{-1})$ has been successfully modeled by the describing-function analysis of Ref. 11. This analysis, coupled with a turbulent flow velocity distribution model, gives reasonable values for the location in the flow of the undulating velocity that drives vortex shedding at the resonator mouth. Having an estimate for this velocity that drives the flow-excited resonance is crucial when employing the describing-function analysis to predict aeroacoustic response of resonators. Additionally, further work needs to be done to quantify the end-correction for wall-mounted resonators in the presence of grazing flow to accurately predict the sounding frequency.

ACKNOWLEDGMENTS

The authors would like to thank the Physics and Astronomy Department at the University of Central Arkansas and the Acoustical Society of America's Robert W. Young Award for undergraduate student research in acoustics for support.

[1]A. Cummings, "Acoustics of a wine bottle," J. Sound Vib. **31**, 331–343 (1973).
[2]J. S. Anderson, "The effect of an air flow on a single side branch Helmholtz resonator in a circular duct," J. Sound Vib. **52**, 423–431 (1977).
[3]S. Elder, "Self-excited depth-mode resonance for a wall-mounted cavity in turbulent flow," J. Acoust. Soc. Am. **64**, 877–890 (1978).
[4]S. A. Elder, "Forced oscillations of a separated shear layer with application to cavity flow-tone effects," J. Acoust. Soc. Am. **67**, 774–781 (1980).
[5]S. A. Elder, T. M. Farabee, and F. C. DeMetz, "Mechanisms of flow-excited cavity tones and low Mach number," J. Acoust. Soc. Am. **72**, 532–549 (1982).
[6]M. S. Howe, "On the Helmholtz resonator," J. Sound Vib. **45**, 427–440 (1976).
[7]M. S. Howe, "The influence of mean shear on unsteady aperture flow, with application to acoustical diffraction and self-sustained cavity oscillations," J. Fluid Mech. **109**, 125–146 (1981).
[8]P. A. Nelson, N. A. Halliwell, and P. E. Doak, "Fluid dynamics of flow excited resonance, part I: Experiment," J. Sound Vib. **78**, 15–38 (1981).
[9]P. A. Nelson, N. A. Halliwell, and P. E. Doak, "Fluid dynamics of flow excited resonance, part II: Flow acoustic interaction," J. Sound Vib. **91**, 375–402 (1983).
[10]T. D. Mast, "Physical theory of narrow-band sounds associated with intracranial aneurysms," Ph.D. dissertation, The Pennsylvania State University, State College, PA, 1993.
[11]T. D. Mast and A. D. Pierce, "Describing-function theory for flow excitation of resonators," J. Acoust. Soc. Am. **97**, 163–172 (1995).
[12]M. Meissner, "The response of a Helmholtz resonator to external excitation. Part I: Acoustically induced resonance," Arch. Acoust. **29**,107–121 (2004).
[13]M. Meissner, "The response of a Helmholtz resonator to external excitation. Part II: Flow-induced resonance," Arch. Acoust. **30**, 57–71 (2005).
[14]H. Kook, "Prediction and control of the interior pressure fluctuations in a flow-excited Helmholtz resonator," Ph.D. dissertation, Purdue University, West Lafayette, IN (1997).
[15]H. Kook and L. Mongeau, "Analysis of the periodic pressure fluctuations induced by flow over a cavity," J. Sound Vib. **251**, 823–846 (2002).
[16]M. Inagaki, O. Murata, and T. Kondoh, "Numerical prediction of fluid-resonant oscillation at low Mach number," AIAA J. **40**, 1823–1829 (2002).
[17]S. Mallick, R. Shock, and V. Yakhot, "Numerical simulation of the excitation of a Helmholtz resonator by a grazing flow," J. Acoust. Soc. Am. **114**, 1833–1840 (2003).
[18]B. Crouse, S. Senthooran, D. Freed, G. Balasubramanian, M. Gleason, M. Puskarz, P. Lew, and L. Mongeau, "Experimental and numerical investigation of a flow-induced cavity resonance with application to automobile buffeting," AIAA Paper No. 2006-2494 (2006).
[19]R. Ma, P. E. Slaboch, and S. C. Morris, "Fluid mechanics of the flow-excited Helmholtz resonator," J. Fluid Mech. **623**, 1–26 (2009).
[20]B. E. Walker and A. F. Charwat, "Correlation of the effects of grazing flow on the impedance of Helmholtz resonators," J. Acoust. Soc. Am. **72**, 550–555 (1982).
[21]A. Cummings, "The response of a resonator under a turbulent boundary layer to a high amplitude non-harmonic sound field," J. Sound Vib. **115**, 321–328 (1987).
[22]K. S. Peat, J. G. Ih, and S. H. Lee, "The acoustic impedance of a circular orifice in grazing mean flow: Comparison with theory," J. Acoust. Soc. Am. **114**, 3076–3086 (2003).
[23]D. Rockwell and E. Naudascher, "Review—self-sustaining oscillations of flow past cavities," J. Fluids Eng. **100**, 152–165 (1978).
[24]R. L. Panton, "Effect of orifice geometry on Helmholtz resonator excitation by grazing flow," AIAA J. **28**, 60–65 (1990).
[25]S. Dequand, X. Lou, J. Willems, and A. Hirschberg, "Helmholtz-like resonator self-sustained oscillations, part 1: Acoustical measurements and analytical models," AIAA J. **41**, 408–415 (2003).
[26]S. Dequand, S. Hulshoff, V. van Kuijk, J. Willems, and A. Hirschberg, "Helmholtz-like resonator self-sustained oscillations, part 2: Detailed flow measurements and numerical simulations," AIAA J. **41**, 416–423 (2003).
[27]J. C. Bruggeman, A. Hirschberg, M. E. H. van Dongen, A. P. J. Wijnands, and J. Gorter, "Self-sustained aero-acoustic pulsations in gas transport systems: Experimental study of the influence of closed side branches," J. Sound Vib. **150**, 371–393 (1991).
[28]P. C. Kriesels, M. C. A. M. Peters, A. Hirschberg, A. P. J. Wijnands, A. Iafrati, G. Riccardi, R. Piva, and J. C. Bruggeman, "High amplitude vortex-induced pulsations in a gas transport system," J. Sound Vib. **184**, 343–368 (1995).
[29]S. Ziada, "A flow visualization study of flow-acoustic coupling at the mouth of a resonant side-branch," J. Fluids Struct. **8**, 391–416 (1994).
[30]S. Ziada and S. Shine, "Strouhal numbers of flow-excited acoustic resonance of closed side branches," J. Fluids Struct. **13**, 127–142 (1999).
[31]W. V. Slaton and J. C. H. Zeegers, "Acoustic power measurements of a damped aeroacoustically driven resonator," J. Acoust. Soc. Am. **118**, 83–91 (2005).
[32]M. Meissner, "Acoustic modes induced by flow in a pipe with two closed side-branches," Appl. Acoust. **63**, 1071–1083 (2002).
[33]P. Oshkai and T. Yan, "Experimental investigation of coaxial side branch resonators," J. Fluids Struct. **24**, 589–603 (2008).
[34]KIMAX Laboratory Glass Drainline. Available from SCHOTT North America, Inc., 555 Taxter Rd., Elmsford, NY 10523.
[35]P. A. Aswatha Narayana and K. N. Seetharamu, *Engineering Fluid Mechanics* (Alpha Science International Ltd., Harrow, UK, 2005), p. 295.
[36]Freescale Semiconductor, Model No. MPX5010, temperature compensated differential pressure sensor. The sensor's response time is 1 ms.
[37]The so-called 5 l resonators are 1/4-in. thick laboratory glass spherical flasks. The actual volume in the flask is 5550 ml.
[38]The factor of $\pi/4$ comes from computing the average distance across the circular side branch opening.
[39]L. E. Kinsler, A. R. Frey, A. B. Coppens, and J. V. Sanders, *Fundamentals of Acoustics*, 4th ed. (Wiley and Sons, Hoboken, NJ, 1999), pp. 284–286.
[40]A. D. Pierce, *Acoustics: An Introduction to Its Physical Principles and Applications*, 3rd ed. (Acoustical Society of America, New York, 1989), p. 350.
[41]Preliminary tests with unequal coaxial Helmholtz resonator neck lengths showed a much weaker aeroacoustic response if any response at all.
[42]R. B. Bird, W. E. Stewart, and E. N. Lightfoot *Transport Phenomena*, 1st ed. (Wiley and Sons, New York, 1960), pp. 153–179.
[43]R. G. Deissler, "Analysis of turbulent heat transfer, mass transfer, and friction in smooth tubes at high Prandtl and Schmidt numbers," Report 1210, National Advisory Committee for Aeronautics (NACA), 1955.